



<b>Publication Year</b>	2016
<b>Acceptance in OA</b>	2020-07-17T10:49:43Z
<b>Title</b>	Optical parametric evaluation model for a broadband high resolution spectrograph at E-ELT (E-ELT HIRES)
<b>Authors</b>	Genoni, Matteo, RIVA, Marco, PARIANI, Giorgio, Aliverti, Matteo, Moschetti, M.
<b>Publisher's version (DOI)</b>	10.1117/12.2233978
<b>Handle</b>	<a href="http://hdl.handle.net/20.500.12386/26479">http://hdl.handle.net/20.500.12386/26479</a>
<b>Serie</b>	PROCEEDINGS OF SPIE
<b>Volume</b>	9911

# PROCEEDINGS OF SPIE

[SPIDigitalLibrary.org/conference-proceedings-of-spie](https://spiedigitallibrary.org/conference-proceedings-of-spie)

## Optical parametric evaluation model for a broadband high resolution spectrograph at E-ELT (E-ELT HIRES)

M. Genoni, M. Riva, G. Pariani, M. Aliverti, M. Moschetti

M. Genoni, M. Riva, G. Pariani, M. Aliverti, M. Moschetti, "Optical parametric evaluation model for a broadband high resolution spectrograph at E-ELT (E-ELT HIRES)," Proc. SPIE 9911, Modeling, Systems Engineering, and Project Management for Astronomy VI, 99112L (8 August 2016); doi: 10.1117/12.2233978

**SPIE.**

Event: SPIE Astronomical Telescopes + Instrumentation, 2016, Edinburgh, United Kingdom

# Optical parametric evaluation model for a broadband high resolution spectrograph at E-ELT (E-ELT HIRES)

M. Genoni<sup>\*ab</sup>, M. Riva<sup>b</sup>, G. Pariani<sup>b</sup>, M. Aliverti<sup>b</sup>, M. Moschetti<sup>b</sup>

<sup>a</sup>Università degli Studi dell' Insubria, Dipartimento di Scienza ed Alta Tecnologia, via Valleggio 11, I-22100 Como, Italy;

<sup>b</sup>Istituto Nazionale di Astrofisica – Osservatorio Astronomico di Brera-Merate, via E. Bianchi 46, I-23807 Merate (LC), Italy

## ABSTRACT

We present the details of a paraxial parametric model of a high resolution spectrograph which can be used as a tool, characterized by good approximation and reliability, at a system engineering level. This model can be exploited to perform a preliminary evaluation of the different parameters as long as different possible architectures of high resolution spectrograph like the one under design for the E-ELT (for the moment called E-ELT HIRES in order to avoid wrong association with the HIRES spectrograph at Keck telescope). The detailed equations flow concerning the first order effects of all the spectrograph components is described; in addition a comparison with the data of a complete physical ESPRESSO spectrograph model is presented as a model proof.

**Keywords:** E-ELT High resolution spectrograph, Spectrograph paraxial model, Field dicing, Echelle cross dispersed spectrograph

## 1. INTRODUCTION: E-ELT HIRES OVERVIEW

The huge photon collecting power of the 39 m primary mirror diameter E-ELT coupled with a High Resolution Spectrograph (this is for the moment called E-ELT HIRES) will allow the European high resolution community to make fundamental discoveries in a wide range of astrophysical areas, outlined by the Science Team of the E-ELT HIRES Initiative<sup>3,4,7</sup>, like:

- The study of Exo-planetary atmospheres and the detection of signatures of life on rocky exo-planets.
- The spectroscopic study of protoplanetary and proto-stellar disks.
- The chemical composition, atmospheres, structures and oscillations of stars.
- The spectroscopic study of the galaxies evolution as well as the three dimensional IGM reconstruction at high redshift.
- Fundamental constants (such as the fine-structure constant  $\alpha$  and the proton-to-electron mass ratio  $\mu$ ) variation and the related cosmology.

The E-ELT will be the largest telescope to observe in visible and infra-red light; the baseline of the optical design (see Fig. 2) is five mirror solution<sup>2</sup>: aspherical (almost paraboloid) primary mirror M1, a convex secondary mirror M2 with 4 m diameter, concave tertiary mirror M3 with 3.75 m diameter, and two flat mirrors (called M4 and M5). These two latter mirrors have the purpose to feed two Nasmyth focal stations and for adaptive optics; below each Nasmyth platform a Gravity Invariant focal station, fed by a steerable and removable mirror (M6), will be located (see Figure 1). In addition the M6 mirror and a Coudè-train relay optics will allow to feed a Coudè focal station, which will be specialized to host instruments requiring very high long term stability in terms of thermal and mechanical perturbations. The telescope structure (rendering shown in Figure 2) will be alt-azimuth type.

\*matteo.genoni@brera.inaf.it;

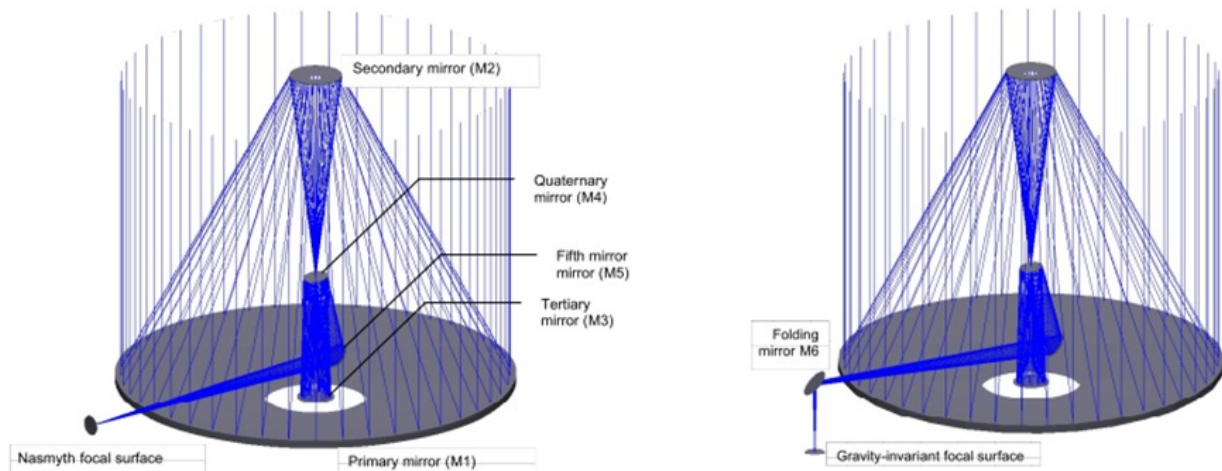


Figure 1. E-ELT optical layout: Nasmyth focus (left) and Gravity invariant focus (right), taken from [2].

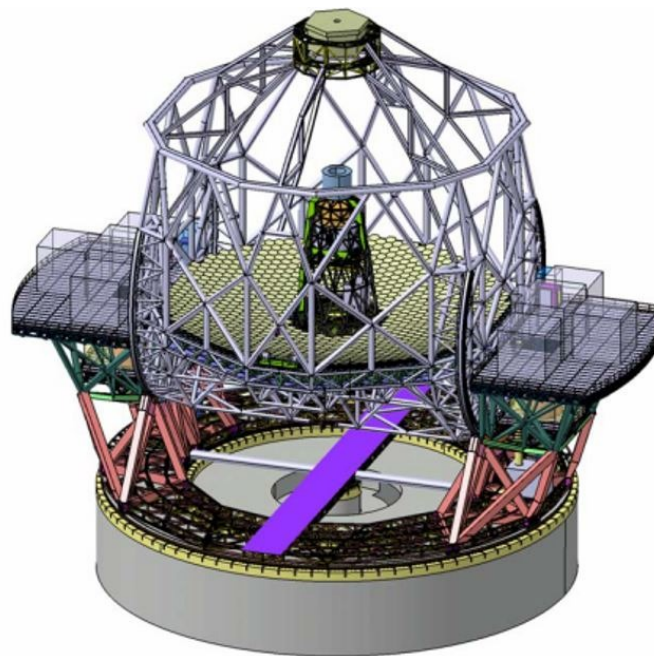


Figure 2. E-ELT structure, rendering, taken from [2].

The E-ELT high resolution spectrograph preliminary architecture concept, proposed by the E-ELT HIRES Initiative working group, is highly modular. It foresees different independent fiber-fed echelle cross-dispersed spectrograph modules optimized for different wavelength bands of the whole spectral coverage of the instrument 330 nm to 2500 nm. The wavelength bands division takes into account the atmospheric transmission profile; different wavelength bands optimized fibers will be used to feed the different modules which, depending on the fibers length-transmission performance<sup>7</sup>, will be located at different distance and operation rooms from the telescope (see Figure 3). The different spectrometers can be divided into two units according to the specific function: the pre-slit unit, a re-imaging system which collects the light from the fiber optics and feeds the spectrometer unit, which has the usual purpose of separate the light into its constitutive wavelengths and then refocus them onto the detector surface. A fore-optics system in

combination with a lenslet array is used to couple the telescope focal plane and the fiber optics<sup>6,7</sup>, which are vertically re-arranged to feed the pre-slit unit. The considered specific technique is called field slicing; in this way the spectrometers entrance slit width is reduced allowing high resolving power performance keeping the components size within manufacturing capabilities.

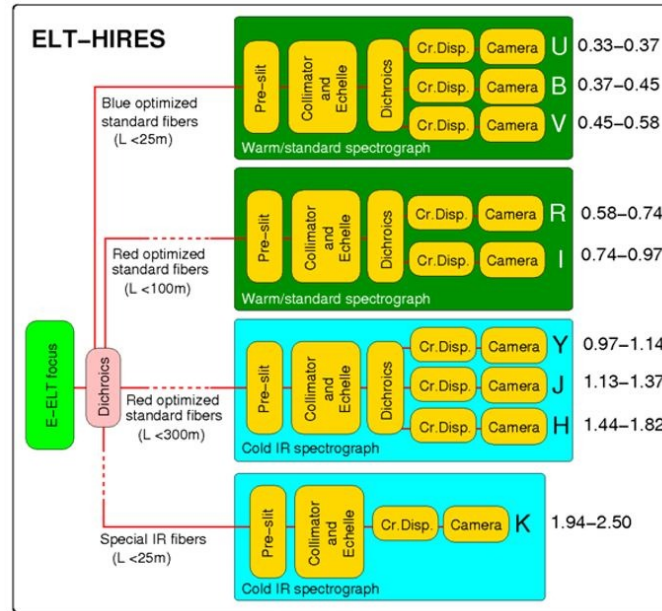


Figure 3. E-ELT HIRES preliminary architecture concept (taken from [7]).

In order to better accomplish the scientific goals, which would be obtained by feeding the spectrograph with different fibers systems with a dedicated interface to the E-ELT telescope, the different modules may also allow different observing modes:

- High Resolution mode (main mode): resolving power  $R = 100000$ , 2 fibers (object and sky) which subtend 0.76 arcsec on sky;
- MOS Medium Resolution mode (ancillary mode): resolving power  $R \geq 10000$ , 10 fibers each looking at different object subtending 0.86 arcsec on sky;
- IFS High resolution mode (ancillary mode): resolving power  $R = 80000$ , 35 fibers for integral field spectroscopy of  $35 \times 49$  milli-arcsec (mas) of field of view.

The main observing mode is a single object mode, in fact the basic scheme foresees two fibers, one fiber for the selected celestial object and the other for sky light subtraction or for calibration purpose, which collect the light from the telescope image plane. As said above the technique used to feed the spectrograph entrance in the proposed architecture is the field dicing, in which each fiber of the optical fibers system is looking at a slightly different part of the object. The optical design of both the pre-slit and spectrometer units of each module foresees the presence of anamorphic effects; in the pre-slit unit the anamorphic x-magnifier effect produced by the re-imager is done to match the light beam F-numbers with the main collimator, while in the spectrometer unit the effects produced by the anamorphic cross-disperser are done to efficiently project the diffracted wavelengths onto the detector surface.

In addition to the Resolving power and wavelength coverage requirements, two other relevant design drivers derived by the E-ELT HIRES Initiative working group are: radial velocity precision  $< 10$  cm/s (related in particular to the exoplanets science) and the signal-to-noise ratio  $\geq 100$ .

## 2. PARAXIAL PARAMETRIC MODEL

In this section we present the details of a flexible paraxial parametric model of the high resolution spectrograph, starting from the assumptions taken into consideration, then describing the equation flow for all the optical components and the related relevant (paraxial) effects.

### 2.1 Model assumptions

According to the paraxial nature of the derived model the aberrations that may be induced by the collimating, focusing optics and other optical elements are not specifically modelled; the other general assumptions are:

- The optic systems that can be exploited to dice the field and to feed the spectrograph entrance are not modelled; only the relevant parameters directly related to the spectrograph design, number of fibers and fiber core diameter, are taken into consideration.
- The anamorphic effects are modelled simply by using different x and y beam re-sizing coefficients; these coefficient are always formally defined as the ratio of the beam size, both for x and y directions, after the effect over the beam size before.
- The echelle grating works in Littrow condition and its efficiency (which is related to the coating that will be proposed, designed and developed in future steps of the project) has been modelled, according to the scalar theory<sup>1</sup>, only for the useful wavelength range determination in each spectral order and not across the different orders.
- The transfer collimator aspect taken into consideration is the beam resizing effect expressed with a coefficient, as done for the anamorphic effects.
- The cross dispersing element efficiency is modelled according to the Bragg condition, but at this level of the model a detailed model of the efficiency trend function of the specific cross dispersed wavelength is not performed.

### 2.2 Model equations flow

Starting from the fixed datum of the telescope diameter  $D_T$  and the angular aperture diameter  $\chi$  of the object image on the telescope focal plane, due to the seeing condition, the number of fibers  $N_f$  used to dice the field and the physical constraint on their working input focal ratio, the fibers core diameter is set as:

$$D_{fib} = \frac{D_T F_{fib}}{\sqrt{N_f}} \frac{\chi}{206265} \quad (1)$$

Setting the main collimator x and y F-ratio, directly related to its design and manufacturing complexity, the pre-slit anamorphic factor and the x and y dimensions of the effective equivalent entrance slit of the spectrometer unit (related to a fiber core) are:

$$PS_{AF} = \frac{F_{coll,Y}}{F_{coll,X}} \quad (2)$$

$$D_{eq-slit,X} = \frac{F_{coll,X}}{F_{fib}} D_{fib} \quad (3)$$

$$D_{eq-slit,Y} = \frac{F_{coll,Y}}{F_{fib}} D_{fib} \quad (4)$$

The total illuminated length of the echelle grating mosaic,  $W$ , required to diffract the whole collimated beam after the main collimator is derived from the imposed resolving power  $R$ , which is a top level requirement, and from the grating blaze angle value  $\delta$  (known from the echelle gratings available on the market):

$$W = \frac{D_{eq-slit,X} R}{2 \sin(\delta) F_{coll,X}} \quad (5)$$

The collimated beam x and y size (after the main collimator first pass) can be expressed then as:

$$d_{coll,X} = W \cos(\delta) \quad (6)$$

$$d_{coll,Y} = \frac{d_{coll,X}}{PS_{AF}} \quad (7)$$

It is possible to derive the required number of echelle gratings ( $N_{grat,X}$  and  $N_{grat,Y}$ ) to form the mosaic from the data on the ruled width,  $Rul_W$  and groove length,  $G_l$ , of the echelle gratings available on the market:

$$N_{grat,X} = \frac{W}{Rul_W} \quad (8)$$

$$N_{grat,Y} = \frac{d_{coll,Y}}{G_l} \quad (9)$$

Through the transfer collimator coefficient the x and y size of the beam, after the transfer collimator, are:

$$d_{TC,X} = d_{coll,X} TC_{coeff} \quad (10)$$

$$d_{TC,Y} = d_{coll,Y} TC_{coeff} \quad (11)$$

The anamorphic effects of the cross disperser are modelled with the coefficients  $XD_{AF,X}$  and  $XD_{AF,Y}$  through which the x and y size of the collimated beam, after the cross disperser itself, at the camera optics input are:

$$d_{XD,X} = d_{TC,X} XD_{AF,X} \quad (12)$$

$$d_{XD,Y} = d_{TC,Y} XD_{AF,Y} \quad (13)$$

The camera optics F-ratios are derived by the spectral and spatial sampling value ( $S_X$  and  $S_Y$ ) and by the pixel size for the available detectors on the market according to the specific wavelength band (optical CCD or IR detectors) as:

$$F_{cam,X} = \frac{d_{pix} S_X}{D_{eq-slit,X}} F_{coll,X} \quad (14)$$

$$F_{cam,Y} = \frac{d_{pix} S_Y}{D_{eq-slit,Y}} F_{coll,Y} \quad (15)$$

So the camera focal length is:

$$f_2 = F_{cam,X} d_{XD,X} = F_{cam,Y} d_{XD,Y} \quad (16)$$

To derive the parameters related to the cross disperser the total linear separation between two consecutive orders on the detector surface,  $\Delta y$  must be set; it has been expressed in terms of the number of fibers, pixel size, required spatial sampling, required separation between object and sky fibers ( $\Delta y'$ ) and separation between consecutive orders ( $\Delta y''$ ):

$$\Delta y = (2N_f S_Y + \Delta y' + \Delta y'') d_{pix} \quad (17)$$

From the cross disperser angular dispersion equation the working angle for the Bragg condition is:

$$\alpha_{cd} = \arctan\left(\frac{\lambda_b}{2} \frac{\Delta y}{f_2 \Delta \lambda_b}\right) \quad (18)$$

where in this case  $\lambda_b$  is the central blaze wave of the specific wavelength band and  $\Delta \lambda_b$  is the difference in wavelengths between the central blaze wave and the consecutive one. From the classical diffraction equation (with the cross disperser working spectral order  $m_{cd} = 1$ ) the cross disperser groove density is:

$$\rho_{cd} = \frac{2 \sin(\alpha_{cd})}{m_{cd} \lambda_b} \quad (19)$$

From the linear dispersion equation the total echellogram central height is then expressed as:

$$\Delta y_{tot,1} = \sum_i (f_2 A_{cd,i} \Delta \lambda_i) \quad (20)$$

where  $A_{cd,i}$  is the cross disperser angular dispersion at the different blaze wavelengths. To model the orders' tilt the tilt angles of the maximum and minimum order at the blaze wavelength are computed as:

$$\tan(\psi(m_{min})) = \frac{A_{cd}(\lambda_b(m_{min}))}{A_{ech}(\lambda_b(m_{min}))} \quad (21)$$

$$\tan(\psi(m_{max})) = \frac{A_{cd}(\lambda_b(m_{max}))}{A_{ech}(\lambda_b(m_{max}))} \quad (22)$$

Then it is possible to compute a first order approximation of the additional vertical portion of the covered detector surface assuming a constant orders tilt and by knowing the effective half width of minimum and maximum order:

$$\Delta y_+(m_{min}) = \tan(\psi(m_{min})) \Delta x_+(m_{min}) \quad (23)$$

$$\Delta y_-(m_{max}) = \tan(\psi(m_{max})) \Delta x_-(m_{max}) \quad (24)$$

where the effective half width of minimum and maximum order are computed according to the linear dispersion in the main dispersion direction on the detector, so similarly to what done in Eq. 20 but now referring to the echelle grating angular dispersion.

In particular, working at high resolution performance and high diffraction orders, the effective maximum and minimum wavelength for each order can be generally expressed as:

$$\lambda_- = \lambda_b \left(1 - \frac{c_-}{m}\right) \quad (25)$$

$$\lambda_+ = \lambda_b \left( 1 + \frac{c_+}{m} \right) \quad (26)$$

Where  $c_-$  and  $c_+$  are two coefficients used to set overlapping (typically 10%) between consecutive diffraction orders, which is required for the reconstruction of the entire spectrum in each band. The total echellogram height on the detector surface is then:

$$\Delta y_{tot,2} = \Delta y_{tot,1} + \Delta y_+(m_{min}) + \Delta y_-(m_{max}) \quad (27)$$

The total echellogram width is due to the total width of the minimum order, computed as the sum of the two effective half width derived from the linear dispersion in the main dispersion direction:

$$\Delta x_{tot,2} = \Delta x_+(m_{min}) + \Delta x_-(m_{min}) \quad (28)$$

Finally the fraction of covered detector surface width and height, by the projected orders of the echellogram, are:

$$\Psi_x = \frac{\Delta x_{tot,2}}{Det_x} \quad (29)$$

$$\Psi_y = \frac{\Delta y_{tot,2}}{Det_y} \quad (30)$$

### 3. MODEL VERIFICATION

The derived parametric paraxial model has been tested and verified doing a comparison with Zemax physical model data of the Echelle SPECTrograph for Rocky Exoplanets and Stable Spectroscopic Observations (ESPRESSO), which will be soon installed on the Very Large Telescope (VLT) placed at Cerro Paranal in Chile. The instrument is a fiber-fed, pupil-sliced, two-arm (blue and red), bench-mounted, cross-dispersed echelle spectrograph, placed in vacuum and in a thermally stabilized environment for very high metrological stability<sup>8</sup>. The full spectral coverage is from 380 to 780 nm, with a cut-off between the two arms at about 525 nm. The spectrograph optical layout is shown in Figure 4.

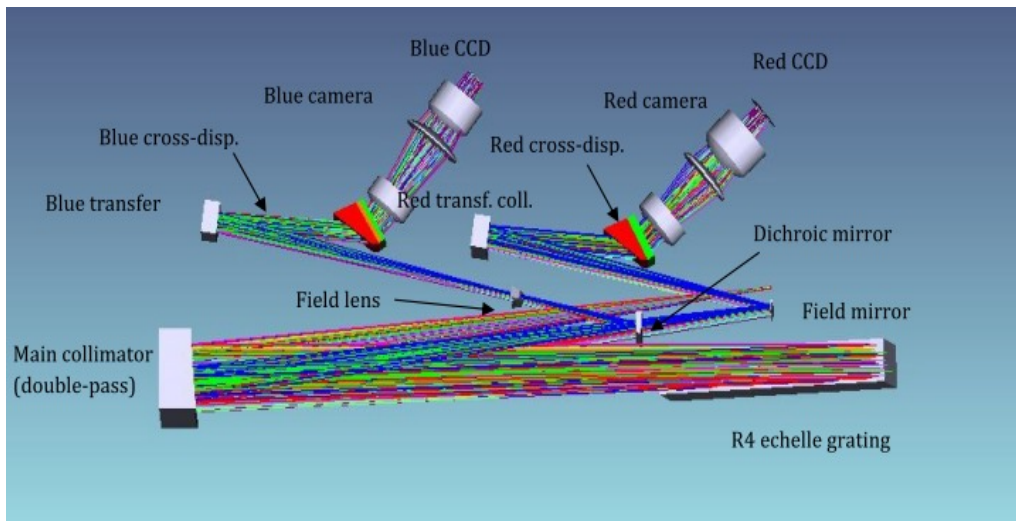


Figure 4. ESPRESSO Spectrograph optical layout: in the figure all the different components of the two arms are shown.

The pupil slicing effect, instead of the field dicing, has been modelled since the ESPRESSO design foresees this technique to meet the resolving power requirement<sup>8</sup>. The pupil slicing effect is given by the Anamorphic Pupil Slicer Unit<sup>9</sup> (APSU), which is in turn the pre-slit unit of ESPRESSO.

Table 1 presents the relevant output parameters, according to a system engineering point of view, related to system complexity and cost issues; in particular the main features of echelle grating and cross disperser, the camera F-numbers are mainly related to complexity issues, while number of echelle gratings and of detector required are mainly related to cost issues.

Table 1. Parametric Paraxial Model results comparison with ESPRESSO Zemax physical model data

Results	Paraxial Parametric Model	ESPRESSO Zemax
$\delta$ [deg]	76	76
$\rho$ [l/mm]	31.6	31.6
$N_{grat,X}$ [-]	3.033	3
$N_{grat,Y}$ [-]	0.978	1
$\alpha_{cd}$ [deg]	20.43	21.24
$\rho_{cd}$ [l/mm]	1478	1500
$F_{cam,X}$ [-]	2.7	2.7
$F_{cam,Y}$ [-]	2.7	2.7
$\Psi_x$ [-]	0.58	0.57
$\Psi_y$ [-]	0.88	0.90

The comparison show a good matching between model and physical results. This is also shown in Figure 5 where the echellograms from the paraxial model and the one from the Zemax model are compared.

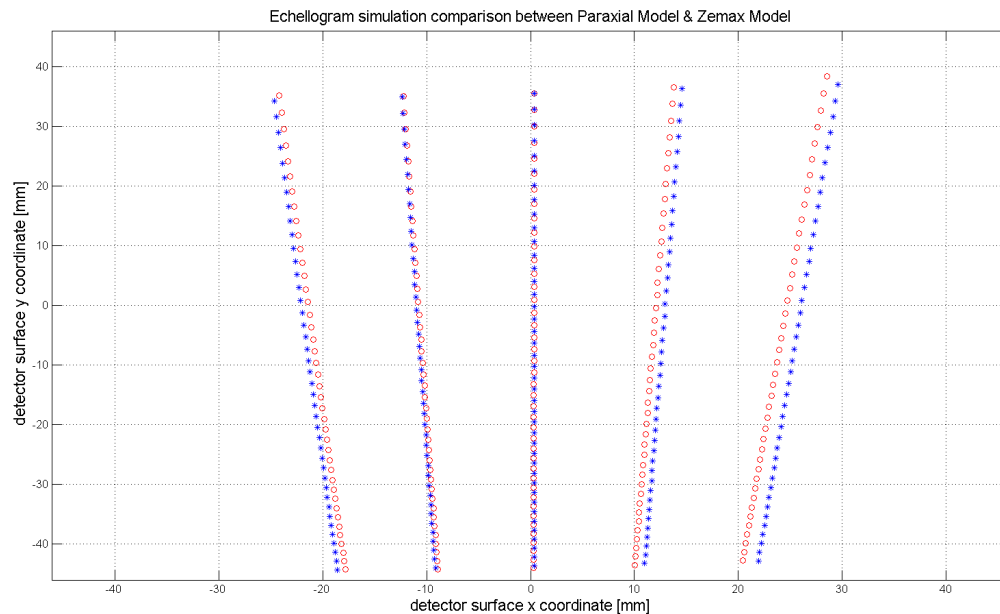


Figure 5. Echellogram simulation comparison between the Paraxial and Zemax physical model. Five wavelengths (including blaze and extreme ones) for each order are shown for a clear representation. Blue star Paraxial model – Red circles Zemax.

#### 4. CONCLUSIONS

A reliable paraxial parametric model for spectrograph design has been derived; it also has a good flexibility in the simulation and evaluation of the wide range of parameters (as well as their interdependencies) involved in the design and architecture definition of such a complex instrument. Focusing on the system engineering level it will be possible to exploit this model in order to easily compare different architecture concepts and to perform different kind of analyses, like input-output parameters sensitivities.

#### REFERENCES

- [1] Schroeder D.J., [Astronomical optics], Academic press, (2007).
- [2] European Southern Observatory, [The E-ELT construction proposal], (2011).
- [3] Maiolino, R., Haehnelt, M., Murphy, M., et al, "A Community Science Case for E-ELT HIRES", arXiv:1310.3163, (2013).
- [4] Origlia, L., Oliva, E., Maiolino, R., et al "SIMPLE: a high-resolution near-infrared spectrometer for the E-ELT", Proc. SPIE 7735, art.id 77352B, 9pp. (2010).
- [5] Kenworthy, M., Parry, I., Taylor, K., "SPIRAL Phase A: Prototype Integral Field Spectrograph for the Anglo-Australian Telescope", PASP 113, p. 215 (2001).
- [6] Parry, I., Bunker, A., Dean, A., et al. "CIRPASS: description, performance and astronomical results", Proc. SPIE 5492, p. 1135 (2004).
- [7] Zerbi, F. M., Bouchy, F., Fynbo, J., et al. "HIRES: The High Resolution Spectrograph for E-ELT", Proc. SPIE 9147, 914723-1, (2014).
- [8] Mégevand, D., Zerbi, F. M., Di Marcantonio, P., "ESPRESSO, the radial velocity machine for the VLT", Proc. SPIE 9147, 91471H, (2014).
- [9] Dell'Agostino, S., Riva, M., Genoni, M., "MMP: multi mini prism device for ESPRESSO APSU, prototyping, and integration", Proc. SPIE 9147, 91475W, (2014).